Applied Microbiology and Biotechnology (2025) 109:116
https://doi.org/10.1007/s00253-025-13501-6

BIOTECHNOLOGICAL PRODUCTS AND PROCESS ENGINEERING

In silico identification of gene targets to enhance C12 fatty acid production in *Escherichia coli*

Paul Matthay[1,2] · Thomas Schalck[1,2] · Kenneth Simoens[3] · Dorien Kerstens[4] · Bert Sels[4] · Natalie Verstraeten[1,2] · Kristel Bernaerts[3] · Jan Michiels[1,2]

Received: 20 December 2024 / Revised: 24 April 2025 / Accepted: 25 April 2025

Abstract

The global interest in fatty acids is steadily rising due to their wealth of industrial potential ranging from cosmetics to biofuels. Unfortunately, certain fatty acids, such as monounsaturated lauric acid with a carbon atom chain length of twelve (C12 fatty acids), cannot be produced cost and energy-efficiently using conventional methods. Biosynthesis using microorganisms can overcome this drawback. However, rewiring a microbe's metabolome for increased production remains challenging. To overcome this, sophisticated genome-wide metabolic network models have become available. These models predict the effect of genetic perturbations on the metabolism, thereby serving as a guide for metabolic pathways optimization. In this work, we used constraint-based modeling in combination with the algorithm Optknock to identify gene deletions in *Escherichia coli* that improve C12 fatty acid production. Nine gene targets were identified that, when deleted, were predicted to increase C12 fatty acid titers. Targets play a role in anaplerotic reactions, amino acid synthesis, carbon metabolism, and cofactor-balancing. Subsequently, we constructed the corresponding (combinatorial) deletion mutants to validate the in silico predictions in vivo. Our highest producer (Δ*maeB* Δ*ndk* Δ*pykA*) reaches a titer of 6.7 mg/L, corresponding to a 7.5-fold increase in C12 fatty acid production. This study demonstrates that model-guided metabolic engineering is a useful tool to improve C12 fatty acid production.

Key points

- *Escherichia coli as a promising biofactory for unsaturated C12 fatty acids.*
- *Optknock to identify non-obvious gene deletions for increased C12 fatty acids.*
- *7.5-fold higher C12 fatty acid production achieved by deleting maeB, ndk, and pykA.*

Keywords Model-guided metabolic engineering · Optknock · *Escherichia coli* · Lauric acid · C12 fatty acids · Oleochemicals

Introduction

Petrochemicals comprise an indispensable part of our everyday life. However, the crude oil reserves from which these valuable compounds originate are not renewable and the use of fossil oils in industrial processes is linked to environmental pollution (Bosco et al. 2005). To facilitate the transition towards a petrol-independent chemical industry, oleochemicals are emerging as promising alternatives to petrochemicals. The latter are derived from fatty acids that are typically harvested from plant fats, including coconut or rapeseed oils (Pfleger et al. 2015). Oleochemicals cover a broad spectrum of industrial applications, ranging from production of pharmaceuticals over bioplastics to biofuels (Kalustian 1985; Zhang et al. 2004; Gow 2009; Sanders 2009). Although

Kristel Bernaerts and Jan Michiels contributed equally as co-senior authors to this work.

✉ Jan Michiels
jan.michiels@kuleuven.be

1 VIB-KU Leuven Center for Microbiology, Kasteelpark Arenberg 20, 3001 Louvain, Belgium

2 KU Leuven Centre of Microbial and Plant Genetics, Kasteelpark Arenberg 20, 3001 Louvain, Belgium

3 Chemical and Biochemical Reactor Engineering and Safety Section, Department of Chemical Engineering, KU Leuven, Celestijnenlaan 200 F, 3001 Louvain, Belgium

4 KU Leuven Center for Sustainable Catalysis and Engineering, Celestijnenlaan 200 F, 3001 Louvain, Belgium

Published online: 08 May 2025

plant-based production methods of oleochemicals do not rely on fossil oils, these processes are not sustainable yet on a large industrial scale since oleochemical-dedicated crops are directly competing with food production (Pfleger et al. 2015). Furthermore, the array of fatty acids (unsaturated side chains or presence of functional groups) is rather limited in plants, upping production costs of these molecules tremendously. A prime example is unsaturated lauric acid (unsaturated C12 fatty acid) (Lu et al. 2017).

Bacterial biosynthesis of C12 fatty acids could overcome these drawbacks and allow industrial production in a sustainable manner. Many species are currently under investigation to produce various high-value biochemicals as microbial synthesis is cost and energy-efficient (Ferrer-Miralles et al. 2009; Baez et al. 2011; Cardoso et al. 2020). Moreover, microbes need less extreme operation conditions compared to physicochemical production setups (Zhang et al. 2016; Cho et al. 2020). However, the utilization of microbes to produce C12 fatty acids represents a balancing act of resource utilization. Identifying genetic strategies that rewire the metabolism towards production without dramatically perturbing growth (biomass) represents a major challenge in metabolic engineering. Traditional strategies for identifying genes that are (in)directly involved in the production pathway of interest comprise experimental screening and manual rational design, but both approaches come with some limitations. The former is linked to expensive and tedious manual experiments. The latter, by contrast, is not very efficient in finding all targets as the complete metabolic network of any cell, even well-studied ones, contains thousands of parameters and variables that need to be considered.

Constraint-based metabolic modellng can overcome those shortcomings. In recent years, comprehensive whole-genome metabolic network models have been developed and experimentally validated that mimic the metabolism of cells. In practice, the constraint-based reconstruction and analysis (COBRA) toolbox offers a convenient platform to streamline description and analysis of whole-genome metabolic models (Heirendt et al. 2019). This has resulted in its widespread use to identify engineering approaches to increase microbial production of various biochemicals, such as an increased glycolic acid production in *Escherichia coli* (Kim et al. 2024a) or vitamin B12 production in *Pseudomonas putida* (Prieto-de Lima et al. 2024).

For metabolic engineering, the COBRA toolbox includes the bi-level optimization algorithm Optknock that accounts for the tradeoff between biomass growth and production of a specific metabolic product (Burgard et al. 2003). This algorithm assists in identifying reactions that, when eliminated from the species' metabolic network, increase the flux through a desired target reaction while retaining a minimally desired biomass growth rate. In early research, the metabolism of *E. coli* has already been modelled with the aim of finding genetic interventions to increase fatty acid production. However, the utilized approaches identified common gene deletion targets (Ranganathan et al. 2012; Lennen and Pfleger 2012).

In this study, we used the COBRA toolbox to rationally design an *E. coli* strain to produce C12 fatty acids. *E. coli* represents an ideal model organism as it has previously successfully been exploited for the production of fatty acids, mainly saturated and unsaturated C16 and C18 fatty acids (Matthay et al. 2023) (Fig. 1). Furthermore, *E. coli* has been engineered to produce a variety of other biomolecules such as syringic acid (Liu et al. 2024) and α,ω-diamines (Kim et al. 2024b), and its entire metabolome has accurately been described in the *i*ML1515 metabolic network model (Monk et al. 2017). This model has already been used to deepen the understanding of 3-hydroxybutyrate production in *E. coli* (Park et al. 2019). Moreover, other, older metabolic network models have successfully been used to facilitate engineering of *E. coli* into dedicated bio-factories for the production of, e.g., amino acids (Pharkya et al. 2003), 1,4-butanediol (Yim et al. 2011), and lactic acid (Fong et al. 2005).

Adding to the choice of *E. coli* as a model organism is that, until now, most engineering efforts on microbial (unsaturated) C12 fatty acid production have focused on *E. coli*, which unfortunately also renders a comparison with other organisms challenging. However, comparing the production levels of monounsaturated fatty acids in general shows a similar production potential of the most common model organisms. Engineered *E. coli* can produce up to 6.6 g/L monounsaturated fatty acids, compared to 10 and 4 g/L in similar conditions by *Saccharomyces cerevisiae* and *Yarrowia lipolytica*, respectively (Ledesma-Amaro et al. 2016; Yu et al. 2018).

As *E. coli* natively does not synthesize medium chain fatty acids, production of C12 fatty acids relies on the expression of exogenous enzymes from other organisms. A prime example of the latter is the thioesterase *BTE* from *Umbellularia californica* which has previously been shown to promote the production of C12 fatty acids in *E. coli* (Voelker and Davies 1994). Since thioesterases do not induce unsaturation in the acyl-chain, but rather stop the elongation, the unsaturation in the C12 fatty acids is potentially induced by the cell's natural machinery, which induces a double bond on the ten-carbon acyl chain intermediate, potentially leading to the production of $C12{:}1^{\Delta 5}$. Exploiting the Optknock algorithm within the COBRA toolbox to remodel the metabolism of *E. coli* expressing *BTE* allowed us to identify potential gene targets that upon deletion were suggested to further increase C12 yields. In silico predictions were validated in vivo following construction of the corresponding knock-out mutants. Validated targets play a role in anaplerotic reactions, aromatic amino acids synthesis central carbon metabolism and co-factor balancing.

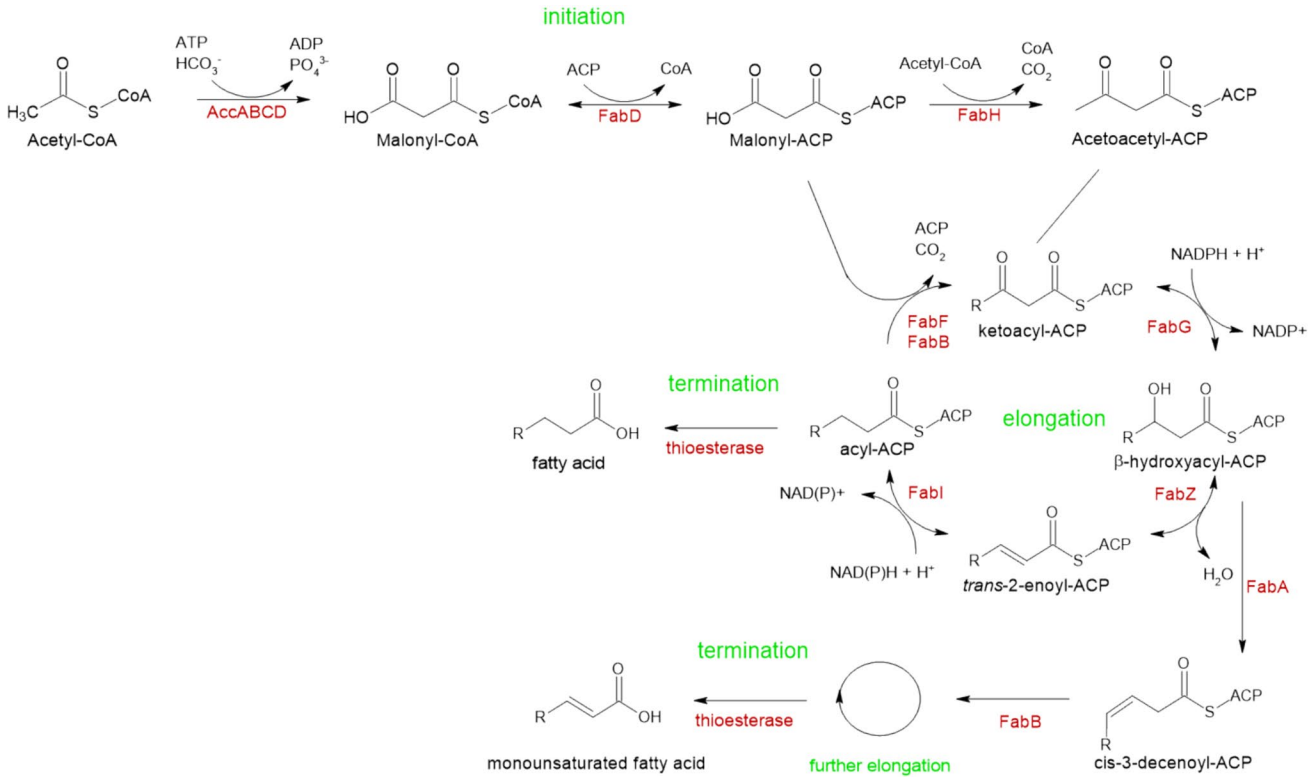

Fig. 1 Schematic overview of the fatty acid biosynthesis in *E. coli*. Enzymes are indicated in red and pathway sections in green. The fatty acid biosynthesis is initiated by converting acetyl-CoA to malonyl-CoA. Subsequently, the latter is functionalized by replacing CoA with an ACP and further converted into acetoacetyl-ACP, which enters the elongation as the first ketoacyl-ACP. The elongation consists of four iterative steps, where each completed cycle adds two carbon atoms to the acyl chain. In detail, ketoacyl-ACP is reduced to hydroxyacyl-ACP, which is hydrated to enoyl-ACP and further reduced to acyl-ACP. This intermediate can either be elongated further by completing another cycle of the fatty acid biosynthesis cycle, or it can be terminated by an acyl-ACP thioesterase, which removes the ACP and releases the free fatty acid. To produce unsaturated fatty acids, the hydroxyacyl-ACP intermediate is dehydrated and isomerized into a cis-enoyl-ACP intermediate to retain the double bond. Thereafter, the ACP-coupled unsaturated fatty acid can be either released by a thioesterase or it can continue one or more cycles similarly to their saturated analogues. *CoA* coenzyme A, *ACP* acyl carrier protein

Materials and methods

Bacterial strains and growth conditions

E. coli BW25113 (NCBI:txid679895) was used throughout this work. Single-gene knock-out mutants were retrieved from the Keio collection (Baba et al. 2006). The Km-resistance cassette was removed using a Flp recombinase that is expressed from the pCP20 plasmid and recognizes FRT sites in the genome (Cherepanov and Wackernagel 1995). Afterwards, the pCP20 plasmid was cured from the mutant by incubation at 42 °C. To create mutants with multiple gene knock-outs, we replaced target genes of interest by a kanamycin cassette flanked by FRT sites using the recombination-enabling plasmid pKD46 (Datsenko and Wanner 2000). This oligo was amplified from the corresponding mutant in the Keio collection (Baba et al. 2006) using the matching primers included in Table 1 and following a previously published protocol (Wilmaerts et al. 2019).

The *BTE* allele was expressed from a tightly-controlled P_{tet} promoter on a vector derived from the Cas9-expressing CRISPR plasmid, pCas9-CR4 (Reisch and Prather 2015). To construct the *BTE* expression vector, the *BTE* gene was synthesized using a BioXp3200 DNA synthesis instrument based on a previously published sequence which was codon optimized for *E. coli* (Lennen et al. 2010). The gene was introduced in the pCas9-CR4 plasmid (Lennen et al. 2011; Reisch and Prather 2015) using Gibson assembly, thereby replacing the *cas9* nuclease gene, including its degradation tag. Primers pCas9-CR4-forward and pCas9-CR4-reverse were used to amplify and create Gibson-compatible overhangs for the pCas9-CR4 plasmid while BTE-forward and BTE-reverse were used to prepare the amplified *BTE* product for Gibson assembly (Table 1). The vector and the insert were mixed using a 1 to 4 mass volume in 10 µL MilliQ water and mixed with 10 µL of NEBuilder Hifi master mix. This mixture was incubated

Table 1 Primers used in this study. Gibson primers were designed using the NEBuilder Hifi tool from SnapGene. Deletion primers were constructed using the NCBI primer designing tool

Primer	Function	Sequence
*deoC*_forward	Primers to construct *deoC* deletion	CTTCCAGCAGCAGGTCATCA
*deoC*_reverse		GTTTATCAGCCGGAGCCAGT
*ldhA*_forward	Primers to construct *ldhA* deletion	TGCATTACCCAACGGCAAAC
*ldhA*_reverse		ACGACATCCAGTTCGCTGAC
*maeB*_forward	Primers to construct *maeB* deletion	GTTGTTTTTCCTGCCCCGAC
*maeB*_reverse		CCCGGATCTTCTTCCACCAC
*acs*_forward	Primers to construct *acs* deletion	TAATCGCCTGCCAGTTCGTT
*acs*_reverse		AACCGCTTTGTTTTTGCCGT
*aroA*_forward	Primers to construct *aroA* deletion	CAACCATTCTTTCCCGTCCG
*aroA*_reverse		GGCCCAGAACGCCTTCAAT
*aroC*_forward	Primers to construct *aroC* deletion	ATTTCTGGCTTCCACAGCGT
*aroC*_reverse		GATCCGCCGCGTCAATGAA
*aroL*_forward	Primers to construct *aroL* deletion	GAAGGCAAAAGCGCGACACAA
*aroL*_reverse		ACATCAGCCCCTTTTGCCAGT
*ndk*_forward	Primers to construct *ndk* deletion	GTGGCACGGTCGTCTTCC
*ndk*_reverse		CCAGTGCCGTACCATTGTTG
*pykA*_forward	Primers to construct *pykA* deletion	TCCATTGGGTAAAAATCTGACACTG
*pykA*_reverse		GCAGGCCAAAGAGATTGTGC
pCas9-CR4-forward	Primers to prepare pCas9-CR4 vector for introduction of *BTE*	TTCGGTTTCCACTCTAGACATAC GGTTAATTCCTCCTATCTTTTGAATTC TTTTCTCTATCACTGATAGGGAG
pCas9-CR4-reverse		TTCGGTTTCCACTCTAGACATAC GGTTAATTCCTCCTATCTTTTGAATTC TTTTCTCTATCACTGATAGGGAG
BTE-forward	Primers to prepare *BTE* to be introduced in pCas9-CR4	GAGAAAAGAATTCAAAAGATAGGAGGAATTAACCATGTGTCTAGAGTG GAAACCGAAACCAAAACT
BTE-reverse		TCAAGGAAATTCAGACTCATGGTTAATTCCTCCTTTAAACACGAGGTTCCG CCGG

at 50 °C for 1 h and transferred to *E. coli* by chemical transformation (Green and Rogers 2013).

For strain construction and storing purposes, the strains were grown in lysogeny broth (LB) containing 10 g/L tryptone, 10 g/L NaCl, and 5 g/L yeast extract. For assaying growth kinetics and fatty acid production, LB and LB supplemented with 10 g/L glucose were used. For stable propagation of plasmids, 30 µg/mL chloramphenicol (BTE) and 100 µg/mL ampicillin (pKD46 and pCP20) were added in the growth broth. For long-term storage, strains were mixed with 25% (v/v) glycerol and kept at – 80 °C.

Quantification of fatty acid production

Strains were incubated in triplicates overnight in tubes with 5 mL LB medium at 37 °C, shaking at 200 rpm (tube dimensions: 27 mL content, 15.5 cm outside length, 1.5 cm diameter). Next, the cells were diluted 100-fold in 5 mL fresh LB medium supplemented with 10 g/L glucose and, if needed, 0–1000 ng/mL anhydrotetracycline to induce BTE expression. After an additional 24-h incubation step, 1 mL of sample, cells and spent medium, was collected for gas chromatography (GC) analysis.

The fatty acid extraction and GC protocol was based on literature (Voelker et al. 1992; Kerstens et al. 2020), but slightly adapted to fit the experimental setup. Each collected 1 mL sample was acidified with 50 µL glacial acetic acid and spiked with 30 µL pentadecanoic acid standard (10 mg/mL). The fatty acids were extracted by adding a 2 mL 1:1 methanol:chloroform mixture and left at room temperature overnight. The lower, organic phase was collected, evaporated using nitrogen, and re-suspended in 2 mL 5% (v/v) H_2SO_4 in methanol. Next, the mixture was incubated for 2 h at 80 °C and, thereafter, 500 µL of 0.9% (w/v) aqueous NaCl solution was added. In order to extract the fatty acids, 500 µL hexane was added and the upper organic phase was collected for GC-FAME analysis. To quantify the fatty acids, 1 µL of the hexane layer sample was injected into a 59:1 split injection system of a Hewlett Packard HP6890 gas chromatograph, equipped with a CP-Sil 88 column (100 m length, 0.25 mm diameter, and 0.2 µm film thickness).

Growth curves

To construct growth curves, overnight cultures were diluted to an OD_{595} of 0.1 and then further diluted 100-fold in LB medium containing 100 ng/mL anhydrotetracycline and possibly 10 g/L glucose. Each well of a honeycomb plate was filled with 200 µL diluted sample. The honeycomb plate was installed in a Bioscreen C device and incubated for 24 h at 37 °C, shaking at 200 rpm to record the OD_{600} every 15 min and analyzed in GraphPad Prism 9.

In silico predictions of beneficial gene knock outs

In silico calculations were performed with the COBRA Toolbox v.3.0 in the Matlab 2022b environment (Heirendt et al. 2019). The simulations were based on the genome-scale reconstruction *i*ML1515 of *E. coli*, which includes 2719 reactions, 1192 metabolites, and 1515 protein structures (Monk et al. 2017). The BTE reaction of interest in *i*ML1515 was present in the model and named FA120 ACPHi while the exchange reaction for C12 fatty acids was named EX_ddca_e. No secretion is imposed. To ensure a flux through FA120 ACPHi, the lower bound was set to 10 mmol gDW^{-1} h^{-1}. Furthermore, all the exchange reactions were upper/lower bounded to mimic rich medium under aerobic growth and glucose as the growth-limiting carbon source, for details see Table S1 and S2. Knock-out mutants were identified using a one-objective strategy (maximization of the flux through FA120 ACPHi) as well as a two-objectives strategy (maximization of C12 fatty acid production and biomass growth).

For the one-objective strategy, deleting a reaction was simulated by setting the lower and upper flux boundary to zero. Next, a flux balance analysis (FBA) was performed to obtain the flux though FA120 ACPHi. This FBA was performed for each model reaction separately, excluding transport and exchange reactions.

For the two-objectives strategy, the bi-level optimization algorithm Optknock was used (Burgard et al. 2003). The input set of candidate reactions was selected by identifying reactions on which FA120 ACPHi has the highest effect. To select those, the flux in FA120 ACPHi was incremented from 10 to 140 mmol gDW^{-1} h^{-1} in steps of 10. For each step, a flux balance analysis was performed and the flux of each single reaction reordered. For each reaction the absolute differences between the steps were summed up, resulting in a value mirroring the effect of BTE on each reaction in the network model, further referred to as C12-values. Next, two Optknock runs were performed in which the growth of the mutants was set to be minimally half of the original strain without deletions. First, the C12-values for each pathway were averaged. The pathways with the highest average C12-value were retained as input for Optknock in which the optimization algorithm was allowed to suggest maximal two deletions. Second, the 50 reactions with the highest C12-value were passed to Optknock, thereby allowing two, three and four deletions.

Results

In silico identification of gene deletions that increase the production of C12 fatty acids in *E. coli*

To discover metabolic genes that upon deletion increase the C12 fatty acid production in *E. coli*, we used the latest genome-wide metabolic network model *i*ML1515 within the COBRA toolbox (Monk et al. 2017; Heirendt et al. 2019). To allow biomass accumulation in the model, we defined a rich medium, consisting both of glucose as the main carbon source and amino acids as nitrogen source and secondary carbon source. *E. coli* does not naturally produce C12 fatty acids, but is transformed into a C12-producer by expressing the plant-derived BTE thioesterase. This enzyme releases fatty acids from the cyclic biosynthesis pathway when compounds reach a carbon chain length of twelve (Voelker and Davies 1994). In silico, this reaction corresponds to the already implemented reaction FA120 ACPHi, EC 3.1.2.21 (a fatty-acyl-ACP hydrolase) in *i*ML1515. The exchange reaction for C12 fatty acids is also included and named EX_ddca_e. Within the model the released C12 fatty acids are exclusively used to be degraded and re-enter the fatty acid biosynthesis. Performing a flux balance analysis in the present solution space results in a zero flux thought FA120 ACPHi. Increasing its flux simulates BTE overexpression, resulting in C12 fatty acid production. While extreme fluxes of BTE completely abolish growth, we were able to distinguish a maximum threshold of 140 mmol gDW^{-1} h^{-1} at which *E. coli* can grow (Fig. 2A).

To identify genes that could have a positive effect on C12 titers when deleted in *E. coli*, two strategies were pursued. The one-objective strategy aims to identify targets that solely improve the flux through FA120 ACPHi, whereas the two-objective strategy predicts targets that not only maximize the flux through FA120 ACPHi but also optimize biomass accumulation.

In the first scenario, we identified beneficial single reaction deletions by performing a flux balance analysis and obtaining the flux through FA120 ACPHi (Fig. 2B). A deletion of each reaction within the *i*ML1515 model was tested by setting the corresponding flux to zero, excluding transport and exchange reactions. This approach revealed four reaction deletions with a beneficial effect on the flux through FA120 ACPHi. The associated genes are *gmk* and *aroACL*. *gmk* encodes an essential guanylate kinase and *aroACL* is an

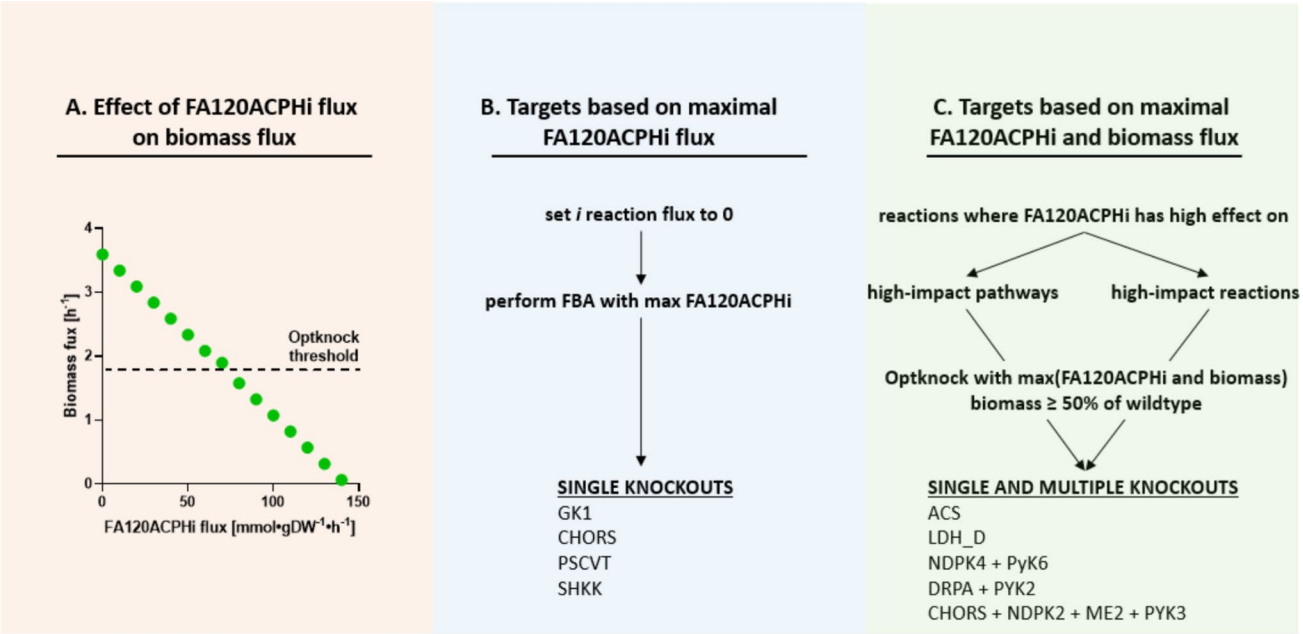

Fig. 2 Schematic overview of computational approaches for increasing the FA120 ACPHi (BTE) flux. **A** Impact of FA120 ACPHi on growth. The lower bound of FA120 ACPHi was increased in a stepwise manner and the biomass flux was determined for each step. **B** Identifying deletion targets based on maximizing FA120 ACPHi with GK1 representing the *E. coli* gene *gmk*, CHORS *aroC*, PSCVT *aroA*, and SHKK *aroL*. **C** Utilization of Optknock to identify gene deletions for optimized FA120 ACPHi and biomass flux with ACS representing the *E. coli* gene *acs*, NDPK4 *adk* and *ndk*, PYK6 *pykA*, LDH-D *ldhA*, DRPA *deoC*, PYK2 *pykA*, CHORS *aroC*, NDPK2 *adk* and *ndk*, ME2 *maeB* and PYK3 *pykA*. Predicted fluxes are listed in Table 2

operon involved in transforming shikimate into chorismate, i.e., a critical reaction in the aromatic amino acid biosynthesis (Rodriguez et al. 2014) (Table S1).

In the second strategy, the Optknock algorithm was applied. This bi-level optimization approach optimizes the flux through FA120 ACPHi, while also ensuring a minimum growth rate. To find candidate knockout reactions, we hypothesized that reactions which are strongly impacted by an increased FA120 ACPHi flux might in turn have a large effect on FA120 ACPHi. This set of reactions was determined by calculating the cumulative effect of an increased FA120 ACPHi for each reaction (excl. transport and exchange reactions). From this list of reactions, two candidate sets were identified. On the one hand, the overall effect for each pathway was computed and all reactions of high average C12-value pathways were used as input. On the other hand, the 50 most affected reactions were subjected to the Optknock algorithm (Fig. 2C). During the optimization process, mutants with one up to four combinatorial knockouts were allowed to be proposed by the Optknock algorithm. The highest allowed combinatorial knockout number was set to four as a higher number would likely lead to unacceptable growth inhibition. Five interesting knockout mutants could be identified (Table 2).

When performing the optimization with reactions from pre-selected pathways, the methodology prioritized the pyruvate metabolism and the nucleotide salvage pathway as theoretical deletion targets to enhance C12 production. Regarding the two-carbon metabolism, deleting *acs*, encoding the acetyl-CoA synthetase, was predicted to increase the flux through FA120 ACPHi 1.5-fold while not affecting growth. Next, knocking out the nucleoside-diphosphate kinase (NDPK4), which belongs to the nucleotide salvage pathway, and anaerobic pyruvate kinase (PYK6), was anticipated to raise the flux through FA120 ACPHi threefold while diminishing growth twofold. PYK6 is encoded by *pykA* and NDPK4 is encoded by *adk* and *ndk* in *E. coli*. When starting with the 50 reactions on which FA120 ACPHi had the highest effect, three Optknock runs were performed with a gradually increasing number of allowed deletions. When only one gene could be eliminated, Optknock proposed to delete *ldhA* which is predicted to increase the flux of FA120 ACPHi 1.5-fold while not disturbing growth. Next, the algorithm suggested to eliminate two genes, *deoC* and *pykA*. Finally, the Optknock-based approach recommended deleting *ndk*, *pykA*, *aroC*, and *maeB* simultaneously when the maximum number of reactions to target was set to four. The corresponding quadruple deletion mutant was expected to have a threefold increase in flux through FA120 ACPHi and to show a twofold reduction in growth (Table 2).

Using both strategies, eight knock-out mutants were prioritized based on nine unique genes (Table 2). The details

Table 2 Optknock predictions for increased flux through FA120 ACPHi compared to the original *BTE* expressing strain with a base flux of 10 mmol·gDW^{-1} h^{-1} and growth rate of 0.96 h^{-1}

*i*ML1515 reaction	Reaction name	Gene in *E. coli*	Flux FA120 ACPHi [mmol gDW^{-1} h^{-1}]	Growth rate [h^{-1}]
ACS	Acetyl CoA synthetase	*acs*	17.8	0.96
NDPK4	Adenylate kinase + nucleoside diphosphate kinase	*adk* and *ndk*	37.89	0.46
PyK6	Pyruvate kinase	*pykA*		
LDH_D	D-lactate dehydrogenase	*ldhA*	16.8574	0.98
DRPA	Deoxyribose-phosphate aldolase	*deoC*	17.14778	0.83
PYK2	Pyruvate kinase	*pykA*		
CHORS	Chorismate synthase	*aroC*	31.6674	0.46
NDPK2	Adenylate kinase + nucleoside diphosphate kinase	*adk* and *ndk*		
ME2	NADP-dependent malic enzyme	*maeB*		
PYK3	Pyruvate kinase	*pykA*		

for each deletion can be found in the supplementary information (Table S1). All identified gene deletions can be categorized in four reaction classes, i.e., anaplerotic reactions, aromatic amino acid synthesis, carbon metabolism and cofactor balancing.

Experimental validation of in silico predictions

To validate the results of the metabolic simulations, we first introduced an anhydrotetracycline-inducible copy of the codon-optimized *BTE* sequence in *E. coli* BW25113 (Baba et al. 2006; Lennen et al. 2011). *BTE* needs to be expressed at an optimal expression level to enhance C12 fatty acid production, since it competes with the native, essential thioesterases on the limited supply of available fatty acid precursors (Lennen et al. 2010; Lennen and Pfleger 2012). Therefore, we determined the optimal anhydrotetracycline inducer concentrations for the P_{tet} expression system. The total fatty acid concentration remained at a stable basal level of 30 mg/L over the full expression range of BTE (Fig. 3A), which is in line with earlier reports and can be attributed to the cells' native thioesterases (Lennen and Pfleger 2012). However, after 24 h of growth, a significant increase in C12 titers was observed at an anhydrotetracycline concentration of 100 ng/mL corresponding to 1.7 mg/L (Fig. 3B). The concentration optimum was further confirmed by testing three representative knock-out mutants (Fig. S1). We were unable to explicitly identify the species of unsaturated C12 fatty acid. Since the unsaturation might be induced by the cells' natural machinery, it could be C12:1$^{\Delta 5}$.

Since our model simulated (C12) fatty acid production in glucose and amino-acid rich context, we selected LB medium to validate our in silico predictions. LB inherently contains plenty of catabolizable amino acids and was further supplemented with 10 g/L of glucose to better mimic glucose-rich growth broth. Quantification of fatty acid production by the BTE-expressing *E. coli* strain in the total broth with and without the addition of 10 g/L glucose revealed a 1.5-fold increase of total fatty acids and a 2.5-fold increase of C12 fatty acids in the presence of excess glucose. However, the level of unsaturated C12 fatty acids was 2.5-fold higher in LB without glucose (Fig. 3C and D).

For in vivo validation, we knocked out the gene targets in the *BTE* expressing *E. coli* strain that, upon deletion, were predicted to improve the C12 fatty acid production in silico. The model reactions NDPK2 and NDPK4 are both linked to *ndk* and *adk*. Since the latter is an essential gene, only *ndk* deletion was considered. In glucose-poor LB medium, the majority of the observed changes are attributed to unsaturated C12 fatty acids (Fig. 4). The Δ*aroA* and Δ*aroC* deletions within the aromatic amino acid synthesis pathway decrease total fatty acid production while leaving the unsaturated C12 fatty acid production intact, thereby increasing the percentage of produced unsaturated C12 fatty acids (Fig. S2). In contrast, deletion of *aroL* increases the C12 fatty acid production threefold while leaving the total fatty acids unchanged. Gene knockouts related to the *E. coli* fermentation pathways (Δ*ldhA* or Δ*acs*) do not improve or even abolish the unsaturated C12 fatty acid production completely. Conversely, the double deletion mutant Δ*ndk* Δ*pykA* shows a threefold increased yield compared to the original strain expressing *BTE*, whereas a Δ*deoC* Δ*pykA* mutant produces 1.7-fold more C12 fatty acids. These results align with the predicted in silico modeling values of 3.7-fold and 1.7-fold, respectively. When *aroC* and *maeB* were also knocked out in the Δ*pykA* Δ*ndk* mutant, the resulting strain, Δ*pykA* Δ*maeB* Δ*aroC* Δ*ndk*, exceeds the in silico estimated threefold production benefit as the quadruple mutant displays a fourfold increase in C12 titers. Moreover, the triple Δ*pykA* Δ*maeB* Δ*ndk* mutant shows an even higher increase of 7.5-fold. The reader is referred to supplementary Fig. S3A for the production based on growth, represented by the OD_{595}.

Growing the strains in LB with 10 g/L glucose leads to a higher percentage of saturated C12 fatty acids and

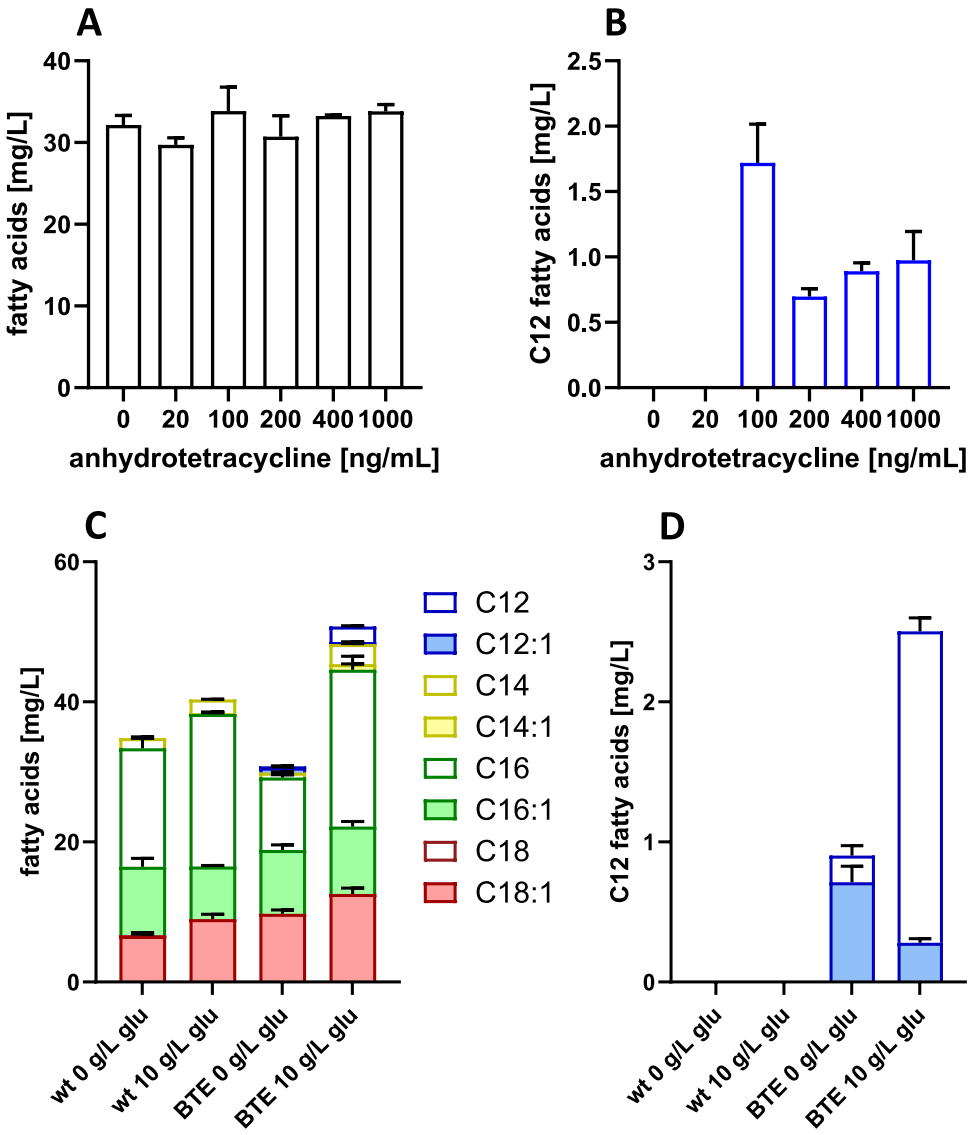

Fig. 3 Optimizing *BTE* expression in *E. coli* for optimal C12 fatty acid production. **A** Total fatty acid and **B** C12 fatty acid production in the *BTE*-overexpressing *E. coli* strain induced with 0–1000 ng/mL anhydrotetracycline and grown for 24 h in LB. **C**, **D** Wild-type *E. coli* (wt) and *E. coli* expressing *BTE* (BTE) were grown for 24 h in LB medium with an inducer concentration of 100 ng/mL and with and without 10 g/L glucose. **C** Total fatty acids and **D** C12 fatty acids (in mg/L) in the wild-type (wt) and *BTE*-overexpressing (BTE) strains in glucose-poor and -rich conditions. Mean values and SEM (standard error of the mean) are shown ($n \geq 3$)

the changes provoked by the gene deletions exclusively affect the saturated C12 fraction instead of the unsaturated one (Fig. 5). From the predicted deletion mutants, only Δ*ldhA* and Δ*aroC* Δ*maeB* Δ*ndk* Δ*pykA* influence C12 and general fatty acid output. All other mutants show no effect and, consequently, do not confirm the predictions of Optknock. Knocking out *ldhA* triggers higher production titers in both total and C12 fatty acids (1.5-fold increase). Moreover, deleting all four genes, *aroC*, *maeB*, *ndk*, and *pykA*, impacts the C12 levels most significantly, reaching a 2.5-fold increment. Importantly, this is the only predicted deletion mutant that raises the C12 fatty acid percentage. Moreover, the best performing mutants is, just as in regular LB, Δ*ndk* Δ*maeB* Δ*pykA*, reaching a C12 fatty acid content of 15% (Fig. S2). Production based on growth, represented by the OD_{595}, is depicted in supplementary Fig. S3B.

Comparing growth in both growth media revealed a lower maximal OD_{600} in the high-glucose condition for all strains. However, the deletion strains did not show any growth defects compared to the wild type, except for Δ*pykA* Δ*ndk* Δ*maeB*. This mutant has a reduced growth rate and maximal OD_{600} irrespective of the glucose concentration (Fig. S4). In terms of C12 production, glucose supplementation improves the total fatty acid output of the mutants about twofold but impedes the production of unsaturated C12 fatty acids. Moreover, the effect of the deletions is more apparent in the non-glucose condition. To illustrate, the best performing mutant in the glucose-rich condition is Δ*pykA* Δ*ndk* Δ*maeB* Δ*aroC* producing 2.5-fold more C12 fatty acids than the wild-type reference (Fig. 5). In contrast, the highest producer in plain LB is Δ*pykA* Δ*ndk* Δ*maeB*, improving C12 titers 7.5-fold (Fig. 4). Finally, regardless of the glucose content, the highest producer is able to produce around 6.7 mg/L

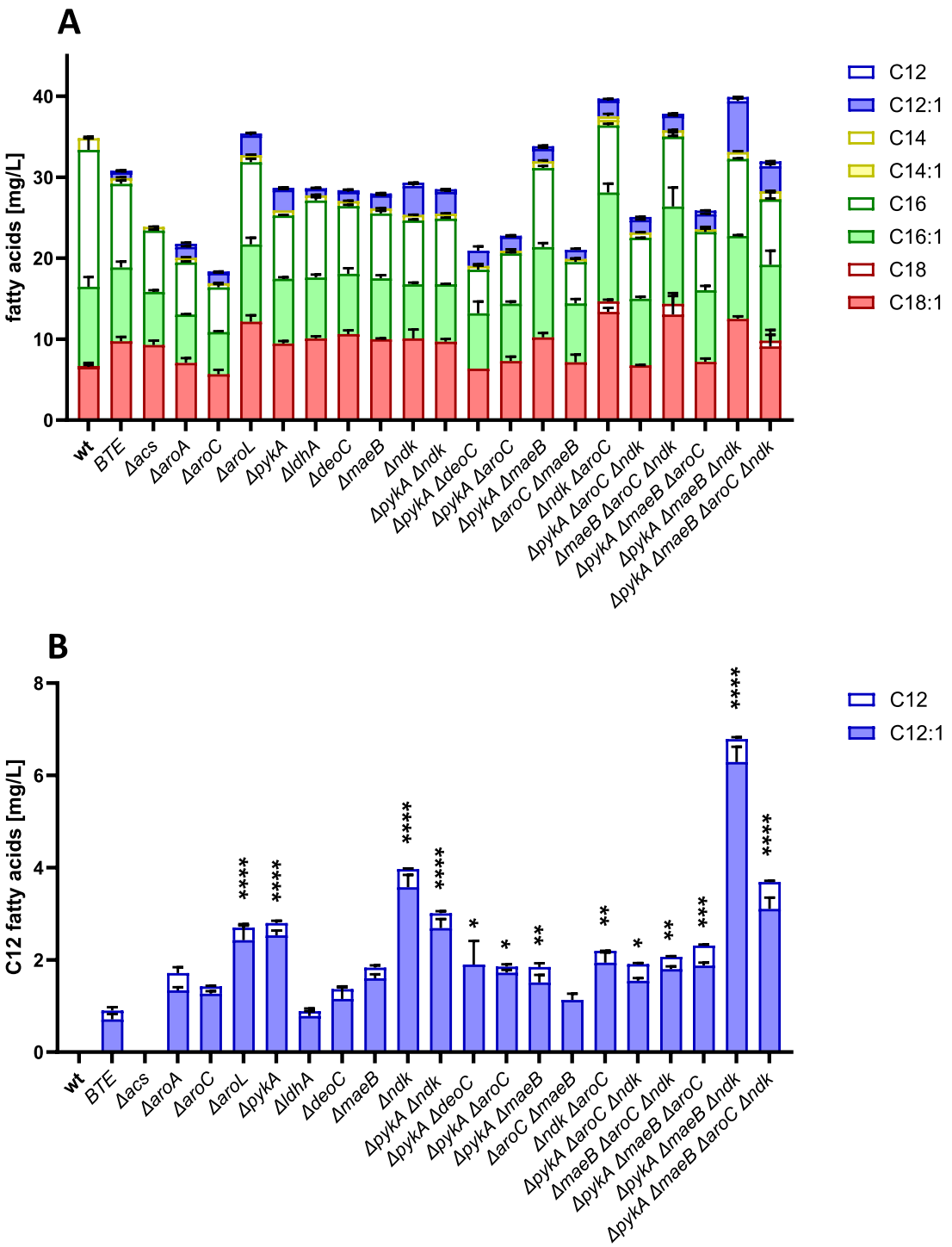

Fig. 4 Effect of the predicted (combinatorial) gene knock-outs on the production of C12 fatty acids in *E. coli*, cultivated in LB. *E. coli* strains (indicated on the x-axis) expressing *BTE* from an anhydrotetracycline-inducible promoter were grown for 24 h in LB medium containing 100 ng/mL of inducer. **A** Total fatty acid production. **B** C12 fatty acid production. Mean values and SEM (standard error of the mean) are shown ($n \geq 3$). Asterisks indicate significant differences calculated with ANOVA in saturated and unsaturated C12 fatty acids compared to *E. coli* BW25113 expressing *BTE*, indicated as BTE (*$p < 0.05$, **$p < 0.01$, ***$p < 0.001$, ****$p < 0.0001$)

of C12 fatty acids. Remarkably, the glucose content in the growth broth heavily determines the degree of unsaturation of C12 fatty acids. While 90% of C12 exists as unsaturated fatty acids in glucose-poor conditions, the opposite is true when the medium is enriched with glucose. In that case, about 90% of the produced C12 fatty acids are saturated.

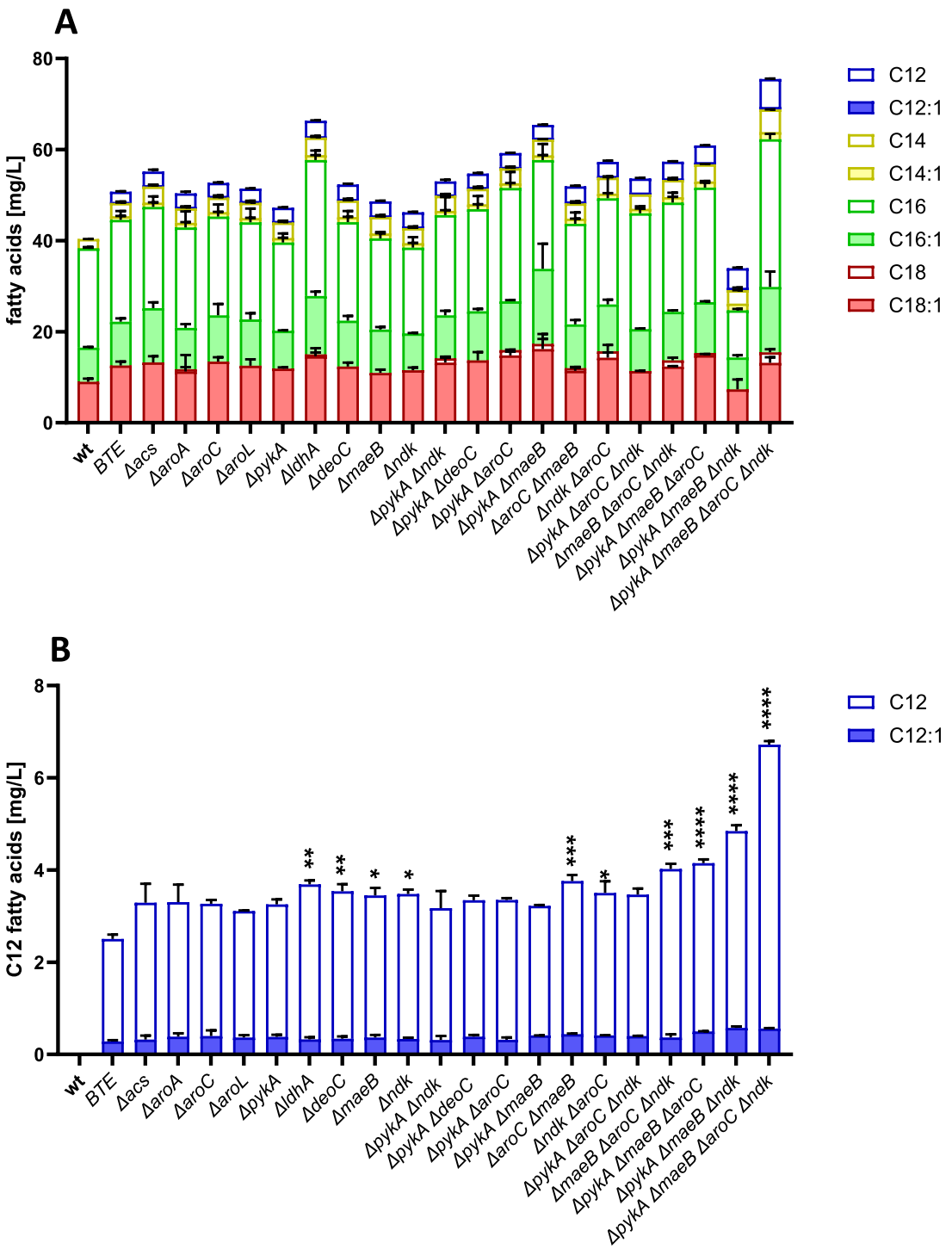

Fig. 5 Effect of the predicted (combinatorial) gene knock-outs on the production of C12 fatty acids in *E. coli*, cultivated in 10 g/L glucose-enriched LB. *E. coli* strains (indicated on the x-axis) expressing *BTE* from an anhydrotetracycline-inducible promoter were grown for 24 h in LB medium containing 10 g/L glucose and 100 ng/mL of inducer. **A** Total fatty acid production. **B** C12 fatty acid production. Mean values and SEM (standard error of the mean) are shown ($n \geq 3$). Asterisks indicate significant differences calculated with ANOVA in saturated and unsaturated C12 fatty acids compared to *E. coli* BW25113 expressing *BTE*, indicated as BTE (*$p < 0.05$, **$p < 0.01$, ***$p < 0.001$, ****$p < 0.0001$)

Discussion

In this work, we constructed *E. coli* strains producing elevated levels of C12 fatty acids in the total fatty acids pool. Combining computational approaches with the latest genome-scale metabolic reconstruction model allowed us to identify non-obvious gene deletion targets that enable a *BTE* overexpressing *E. coli* strain to redirect its carbon fluxes toward non-native C12 fatty acids. Of special interest are the conditions found that showed an increase in the industrial sought-after unsaturated C12 fatty acids. These compounds can be used to produce bioplastics such as nylon (de Leeuw et al. 2019) and find applications in the food and pharmaceutical industry due to their antibacterial and antifungal effects (Fernandez-Lopez 2005; Chandrasekaran et al. 2008). The discovered C12 fatty acid-promoting deletions can be roughly grouped into pathways that are linked to anaplerotic reactions, aromatic amino acid metabolism, central carbon metabolism, and cofactor balancing. Interestingly, overexpression of *acs* has previously been shown to increase fatty acid production sevenfold (Xiao et al. 2013). To the best of our knowledge, other targets identified in this study have never been implicated in fatty acid production.

After completing the metabolic modeling, we introduced the deletions that were suggested by the computational approach in *E. coli* to validate the modeling results in lab-scale production. Deletion strains were tested on their fatty acid production in glucose-poor and -rich LB media. In general, addition of 10 g/L glucose was shown to increase fatty acid production while simultaneously lowering maximal growth (Fig. S4). The latter can be attributed to the rapid metabolization of high levels of glucose, leading to the massive accumulation of various byproducts that hinder growth (Bren et al. 2016; Muenwongtham et al. 2022).

Within each environment, we could identify gene deletions that increase the production of C12 fatty acids, supporting the computational approach. Overall, high glucose concentrations result in increased production of fatty acids in all mutants as well as the BTE control strain where extra glucose elicits a twofold increase in produced fatty acids (Fig. 3). However, unsaturated C12 fatty acid levels are lower in high-glucose conditions. Importantly, both pyruvate and the fatty acid precursor acetyl-CoA (Fig. 1) are provided from different pathways, depending on the glucose content. Plain LB predominantly contains amino acids that are catabolized into pyruvate and glyceraldehyde-3 phosphate which, in turn, trigger the gluconeogenesis pathway (Sezonov et al. 2007; Peskov et al. 2012). In the presence of excess glucose, however, *E. coli* activates the (upper) glycolysis to consume its preferred sugar source, thereby producing pyruvate and other downstream metabolites (Li et al. 2014).

Interestingly, our results indicate that the addition of glucose potentially changes the expression of genes related to the production of (unsaturated) fatty acids. Comparing gene expression in rich and minimal medium revealed that expression of most genes involved in fatty acid biosynthesis is significantly elevated in rich medium (Tao et al. 1999). In another study, different glucose levels in minimal medium were tested showing that expression of *fabZ* and *fabB* decreases slightly with additional glucose, while *fadR* and *fabA* expression levels remain unchanged (Veit et al. 2007). FabB and FabZ are both essential for the production of unsaturated fatty acids and additional glucose might reduce their expression, resulting in a lower production of unsaturated fatty acids (Jeon 2012; Lee et al. 2013). Unfortunately, no expression profiles are described utilizing LB with different glucose concentrations. In future research, expression levels in LB with and without glucose should be evaluated.

Related to the anaplerotic reactions that provide intermediates for the essential TCA cycle, the Δ*ldhA* mutant shows no effect in LB but a small increase when glucose is provided (Figs. 4 and 5). The NAD^+-dependent lactate dehydrogenase, LdhA, catalyzes the reversible reaction between lactate and pyruvate (Zhao et al. 2019). Deleting *ldhA* is expected to accumulate acetate, ethanol, and formate, and to reduce growth and glucose consumption (Kabir et al. 2005; De Mey et al. 2007). Furthermore, Δ*ldhA* enhances the expression of *pck* (phosphoenolpyruvate carboxykinase) while inhibiting *ppc* (phosphoenolpyruvate carboxylase) (Kabir et al. 2005). The former catalyzes the reaction of oxaloacetate toward phosphoenolpyruvate, while the latter catalyzes the reverse reaction. Consequently, Δ*ldhA* is expected to result in an increased availability of phosphoenolpyruvate for the synthesis of acetyl-CoA (Kabir et al. 2005; De Mey et al. 2007). The next anaplerotic target, *maeB*, only favors C12 fatty acid production slightly when knocked out in the glucose-rich condition (Figs. 4 and 5). The encoded malate dehydrogenase turns malate into pyruvate in a reversible reaction with a preference toward pyruvate (Wang et al. 2007; Bologna et al. 2007). With an increased glucose concentration, increased levels of pyruvate are present, resulting in malate dehydrogenase reacting on pyruvate, slightly depleting the pyruvate pool. Finally, removing *pykA* improves C12 fatty acid production by a factor of three in LB. No effect is observed when glucose is added (Figs. 4 and 5). The encoded pyruvate kinase catalyzes the irreversible formation of pyruvate from phosphoenolpyruvate at the gain of one ATP. The reaction proceeds downstream of the glycolysis and as a consequence, supplementation of glucose might provide enough flux toward pyruvate and phosphoenolpyruvate and available ATP, diminishing the importance of *pykA* in glucose-rich environments. However, deletion of *pykA* was shown to increase intracellular ATP, in addition

to decreasing acetate formation and available NADPH (Xie et al. 2014; Zhao et al. 2017).

Single deletions in *aroACL* were predicted to be beneficial when solely maximizing the FA120 ACPhi flux. In addition, the in silico predicted beneficial gene deletions of *aroA* and *aroC* are essential for growth in minimal medium (Díaz et al. 2001). When grown in LB, all mutants show a sharp increase in C12 fatty acid percentages (Fig. S2), while only Δ*aroL* results in an increase of the absolute level of the C12 fatty acid (Fig. 4). Knocking out *aroAC* shuts down aromatic amino acid synthesis (Joyce et al. 2006; Jin et al. 2007), whereas the *aroL* deletion can be partially complemented by *aroK*, which has a lower affinity for shikimate (Millar et al. 1986; Whipp and Pittard 1995). In LB, the aromatic amino acid synthesis seems to be (indirectly) involved in fatty acid synthesis, since compared to the wild type, the corresponding Δ*aroA*, Δ*aroC*, and Δ*aroL* mutants produce lower or equal amounts of fatty acids. It is likely that the aromatic amino acids are recycled in the carbon metabolism and are involved in necessary cofactor synthesis (Díaz et al. 2001). Furthermore, supplementing glucose does not elicit higher C12 fatty acid levels in the three single mutants. In this case, the presence of glucose turns aromatic amino acids redundant as carbon source.

Regarding the central metabolism, knocking out *acs* in LB disrupts C12 fatty acid production and diminishes the total fatty acid yield. The encoded acetyl-CoA synthetase can recycle acetate, which is a byproduct of glycolysis, into the fatty acid biosynthesis pathway by converting it into acetyl-CoA (De Mey et al. 2007) (Fig. 1). Contrary to the prediction, Δ*acs* shows no effect in glucose-rich environments, most likely because pyruvate and acetyl-CoA are produced from the glycolysis in sufficiently large amounts (Figs. 4 and 5). The second central metabolism-associated target, *deoC*, only increases fatty acid production in glucose-rich conditions when deleted (Figs. 4 and 5). *deoC* encodes the deoxyribose-phosphate aldolase and performs the reversible reaction of 2-glyceraldehyde-3 phosphate toward 2-deoxy-D-ribose-5P. Deleting the corresponding gene might cause a higher level of available 2-glyceraldehyde-3 phosphate and acetaldehyde that may ultimately be converted into the fatty acid biosynthesis precursor, acetyl-CoA, through the central carbon metabolism (DeSantis et al. 2003).

Of all single-gene deletions, knocking out *ndk* contributes the most to fatty acid production in LB and the resulting mutant yields titers that can only be surpassed by the highest producer Δ*maeB* Δ*ndk* Δ*pykA* (Fig. 4). This observation turned out to be present only in glucose-poor environments since the impact of adding glucose on production is very limited (Fig. 5). The nucleoside diphosphate kinase encoded by *ndk* is involved in providing sufficient energy carriers to the cell (Lu et al. 1995). *adk* is the essential homolog of *ndk*, and can compensate for it when deleted (Lu and Inouye 1996). Having access to enough cellular energy is crucial for C12 fatty acid synthesis, because production of one molecule of C12 requires, besides ten NADPH reducing equivalents, five ATP molecules (Janßen and Steinbüchel 2014). *ndk* uses ATP to transfer the third phosphate group toward another energy carrier. Consequently, removing *ndk* is expected to lead to an increased level of available ATP that can be used in the fatty acid biosynthesis (Roisin and Kepes 1978).

Despite the single deletions having a strong effect on C12 fatty acid production, the triple mutant Δ*maeB* Δ*ndk* Δ*pykA* displays highest production levels. In LB supplemented with glucose, production levels further increase by knocking out *aroC*, resulting in the quadruple mutant Δ*aroC* Δ*maeB* Δ*ndk* Δ*pykA* (Figs. 4 and 5). Apparently, in LB the synergetic effect of more ATP (Δ*ndk* and Δ*pykA*) and pyruvate (Δ*maeB*) leads to increased levels of C12 fatty acids, but the additional deactivation of the aromatic amino acid biosynthesis results in less (C12) fatty acids.

Two things are important to note for this study. First, constraint-based metabolic modeling has inherent limitations which could result in false-positive hits. Despite *i*ML1515 being the most complete metabolic network model of *E. coli* to date, stoichiometric models do not take into account kinetic aspects, phenomena like diauxic growth, and transcriptional and translational regulations (Monk et al. 2017). In our study, for example, the possible re-uptake of acetate that can be formed on glucose is not modelled but can be present in the experiments. Despite those shortcomings, we were able to identify beneficial deletion targets by looking at the general C12 fatty acid production in the model. Second, in this study we used the common lab strain *E. coli* BW25113 to follow the in silico simulation as closely as possible. As a consequence, the titers achieved in this study are far below the ones that could potentially be reached using a highly engineered industrial *E. coli* strain. For example, by increasing BTE solubility and blocking fatty acid degradation, C12 fatty acid titers of 1.9 g/L have previously been reached (Jindra et al. 2023). This is considerably higher than the yield of 8 mg/L presented here. It remains to be investigated if transferring the mutations identified in this work to a highly engineered industrial strain would further increase C12 fatty acid production.

To conclude, we used constraint-based modeling to identify deletion targets that rewire the metabolism of *E. coli* toward higher C12 fatty acid production. First, *BTE* was introduced and expressed in *E. coli* to enable the cells to produce C12 fatty acids. Next, theoretically beneficial deletion targets were identified assuming that reactions affected by *BTE* have, in turn, an effect on BTE. Under this assumption, eight deletion mutant strains were proposed based on nine different gene deletions. Upon in vivo validation, the fatty acid production of the proposed

mutants was quantified after growth in LB medium and LB medium supplemented with glucose. The presence of glucose allows for efficient synthesis of acetyl-CoA and other essential metabolites, which translates into a twofold increase in fatty acid production in most deletion strains. In addition, strains grown in LB medium show a higher production of unsaturated C12 fatty acids, accounting for a fraction of 90% in the C12 fatty acids pool. Moreover, the highest C12 fatty acid producers are Δ*maeB* Δ*ndk* Δ*pykA* and Δ*maeB* Δ*ndk* Δ*pykA* Δ*aroC* cultivated in glucose-poor or-rich environments, respectively, and both reaching a titer of about 6.7 mg/L. In addition, Δ*maeB* Δ*ndk* Δ*pykA* shows a 7.5-fold increase in production, which is the highest reported increase in literature to the best of our knowledge. Our work demonstrates that constraint-based modeling is a valuable asset to discover novel genetic engineering targets for strain optimization. Thorough optimization of medium composition and processing conditions (e.g., fed-batch cultivation) are expected to improve the obtained yields even further.

Supplementary Information The online version contains supplementary material available at https://doi.org/10.1007/s00253-025-13501-6.

Authors contribution PM, NV, KB, BS, and JM conceived and designed the research. PM conducted the modeling under the guidance of KB. PM conducted experiments and analyzed the data. KS, KB, BS, and DK supported in the analyses. PM, TS, NV, KB, and JM wrote the manuscript. All authors read, edited and approved the manuscript.

Funding This work was supported by grants from the FWO (Research Foundation Flanders: grant S001421 N) and the VIB (Flemish Institute for Biotechnology: core financing and Tech Watch New Technology funding).

Data availability The datasets used and/or analyzed during the current study are available from the corresponding author on reasonable request.

Declarations

Ethical statement This article does not contain any studies with human participants or animals performed by any of the authors.

Competing interests The authors declare no competing interests.

References

Baba T, Ara T, Hasegawa M, Takai Y, Okumura Y, Baba M, Datsenko KA, Tomita M, Wanner BL, Mori H (2006) Construction of *Escherichia coli* K-12 in-frame, single-gene knockout mutants: The Keio collection. Mol Syst Biol 2. https://doi.org/10.1038/msb4100050

Baez A, Cho K-M, Liao JC (2011) High-flux isobutanol production using engineered *Escherichia coli*: a bioreactor study with *in situ* product removal. Appl Microbiol Biot 90:1681–1690. https://doi.org/10.1007/s00253-011-3173-y

Bologna FP, Andreo CS, Drincovich MF (2007) *Escherichia coli* malic enzymes: two isoforms with substantial differences in kinetic properties, metabolic regulation, and structure. J Bacteriol 189:5937–5946. https://doi.org/10.1128/JB.00428-07

Bosco ML, Varrica D, Dongarrà G (2005) Case study: Inorganic pollutants associated with particulate matter from an area near a petrochemical plant. Environ Res 99:18–30. https://doi.org/10.1016/j.envres.2004.09.011

Bren A, Park JO, Towbin BD, Dekel E, Rabinowitz JD, Alon U (2016) Glucose becomes one of the worst carbon sources for *E. coli* on poor nitrogen sources due to suboptimal levels of cAMP. Sci Rep 6:24834. https://doi.org/10.1038/srep24834

Burgard AP, Pharkya P, Maranas CD (2003) Optknock: a bilevel programming framework for identifying gene knockout strategies for microbial strain optimization. Biotechnol Bioeng 84:647–657. https://doi.org/10.1002/bit.10803

Cardoso VM, Campani G, Santos MP, Silva GG, Pires MC, Gonçalves VM, de C. Giordano R, Sargo CR, Horta ACL, Zangirolami TC (2020) Cost analysis based on bioreactor cultivation conditions: production of a soluble recombinant protein using *Escherichia coli* BL21(DE3). BiotechnolRep 26:e00441. https://doi.org/10.1016/j.btre.2020.e00441

Chandrasekaran M, Kannathasan K, Venkatesalu V (2008) Antimicrobial activity of fatty acid methyl esters of some members of *Chenopodiaceae*. Z Naturforsch C 63:331–336. https://doi.org/10.1515/znc-2008-5-604

Cherepanov PP, Wackernagel W (1995) Gene disruption in *Escherichia coli*: Tc^R and Km^R cassettes with the option of Flp-catalyzed excision of the antibiotic-resistance determinant. Gene 158:9–14. https://doi.org/10.1016/0378-1119(95)00193-A

Cho IJ, Choi KR, Lee SY (2020) Microbial production of fatty acids and derivative chemicals. Curr Opin Biotech 65:129–141. https://doi.org/10.1016/j.copbio.2020.02.006

Datsenko KA, Wanner BL (2000) One-step inactivation of chromosomal genes in *Escherichia coli* K-12 using PCR products. P Natl A Sci 97:6640–6645. https://doi.org/10.1073/pnas.120163297

de Leeuw KD, Buisman CJN, Strik DPBTB (2019) Branched medium chain fatty acids: Iso-caproate formation from isobutyrate broadens the product spectrum for microbial chain elongation. Environ Sci Technol 53:7704–7713. https://doi.org/10.1021/acs.est.8b07256

De Mey M, De Maeseneire S, Soetaert W, Vandamme E (2007) Minimizing acetate formation in *E. coli* fermentations. J Ind Microbiol Biot 34:689–700. https://doi.org/10.1007/s10295-007-0244-2

DeSantis G, Liu J, Clark DP, Heine A, Wilson IA, Wong C-H (2003) Structure-based mutagenesis approaches toward expanding the substrate specificity of D-2-Deoxyribose-5-phosphate aldolase. Bioorgan Med Chem 11:43–52. https://doi.org/10.1016/S0968-0896(02)00429-7

Díaz E, Ferrández A, Prieto MA, García JL (2001) Biodegradation of aromatic compounds by *Escherichia coli*. Microbiol Mol Biol Rev 65:523–569. https://doi.org/10.1128/MMBR.65.4.523-569.2001

Fernandez-Lopez R (2005) Unsaturated fatty acids are inhibitors of bacterial conjugation. Microbiol 151:3517–3526. https://doi.org/10.1099/mic.0.28216-0

Ferrer-Miralles N, Domingo-Espín J, Corchero J, Vázquez E, Villaverde A (2009) Microbial factories for recombinant pharmaceuticals. Microb Cell Fact 8:17. https://doi.org/10.1186/1475-2859-8-17

Fong SS, Burgard AP, Herring CD, Knight EM, Blattner FR, Maranas CD, Palsson BO (2005) In-silico design and adaptive evolution of *Escherichia coli* for production of lactic acid. Biotechnol Bioeng 91:643–648. https://doi.org/10.1002/bit.20542

Gow G (2009) Lubricating Grease. In: Mortier RM, Fox MF, Orszulik ST (eds) Chemistry and technology of lubricants. Springer, Netherlands, Dordrecht, pp 411–432

Green R, Rogers EJ (2013) Transformation of chemically competent *E. coli*. Method Enzymol. Elsevier, pp 329–336

Heirendt L, Arreckx S, Pfau T, Mendoza SN, Richelle A, Heinken A, Haraldsdóttir HS, Wachowiak J, Keating SM, Vlasov V, Magnusdóttir S, Ng CY, Preciat G, Žagare A, Chan SHJ, Aurich MK, Clancy CM, Modamio J, Sauls JT, Noronha A, Bordbar A, Cousins B, El Assal DC, Valcarcel LV, Apaolaza I, Ghaderi S, Ahookhosh M, Ben Guebila M, Kostromins A, Sompairac N, Le HM, Ma D, Sun Y, Wang L, Yurkovich JT, Oliveira MAP, Vuong PT, El Assal LP, Kuperstein I, Zinovyev A, Hinton HS, Bryant WA, Aragón Artacho FJ, Planes FJ, Stalidzans E, Maass A, Vempala S, Hucka M, Saunders MA, Maranas CD, Lewis NE, Sauter T, Palsson BØ, Thiele I, Fleming RMT (2019) Creation and analysis of biochemical constraint-based models using the COBRA Toolbox vol 3.0. Nat Protoc 14:639–702. https://doi.org/10.1038/s41596-018-0098-2

Janßen H, Steinbüchel A (2014) Fatty acid synthesis in *Escherichia coli* and its applications towards the production of fatty acid based biofuels. Biotechnol Biofuels 7:7. https://doi.org/10.1186/1754-6834-7-7

Jeon E (2012) Improved production of long-chain fatty acid in *Escherichia coli* by an engineering elongation cycle during fatty acid synthesis (FAS) through genetic manipulation. J Microbiol Biotechnol 22:990–999. https://doi.org/10.4014/jmb.1112.12057

Jin D, Lu W, Ping S, Zhang W, Chen J, Dun B, Ma R, Zhao Z, Sha J, Li L, Yang Z, Chen M, Lin M (2007) Identification of a new gene encoding EPSPS with high glyphosate resistance from the metagenomic library. Curr Microbiol 55:350–355. https://doi.org/10.1007/s00284-007-0268-x

Jindra MA, Choe K, Chowdhury R, Kong R, Ghaffari S, Sweedler JV, Pfleger BF (2023) Evaluation of strategies to narrow the product chain-length distribution of microbially synthesized free fatty acids. Metab Eng 77:21–31. https://doi.org/10.1016/j.ymben.2023.02.012

Joyce AR, Reed JL, White A, Edwards R, Osterman A, Baba T, Mori H, Lesely SA, Palsson BØ, Agarwalla S (2006) Experimental and computational assessment of conditionally essential genes in *Escherichia coli*. J Bacteriol 188:8259–8271. https://doi.org/10.1128/JB.00740-06

Kabir MdM, Ho PY, Shimizu K (2005) Effect of *ldhA* gene deletion on the metabolism of *Escherichia coli* based on gene expression, enzyme activities, intracellular metabolite concentrations, and metabolic flux distribution. Biochem Eng J 26:1–11. https://doi.org/10.1016/j.bej.2005.05.010

Kalustian P (1985) Pharmaceutical and cosmetic uses of palm and lauric products. J Am Oil Chem Society 62:431–433. https://doi.org/10.1007/BF02541417

Kerstens D, Smeyers B, Van Waeyenberg J, Zhang Q, Yu J, Sels BF (2020) State of the art and perspectives of hierarchical zeolites: practical overview of synthesis methods and use in catalysis. Adv Mater 32:2004690. https://doi.org/10.1002/adma.202004690

Kim J, Kim Y-B, Kim J-Y, Seo M-J, Yeom S-J, Sung BH (2024a) Investigation of bottleneck enzyme through flux balance analysis to improve glycolic acid production in *Escherichia coli*. J Microbiol 62:1023–1033. https://doi.org/10.1007/s12275-024-00175-4

Kim YC, Yoo H-W, Park BG, Sarak S, Hahn J-S, Kim B-G, Yun H (2024b) One-pot biocatalytic route from alkanes to α, ω-diamines by whole-cell consortia of engineered *Yarrowia lipolytic*a and *Escherichia col*i. ACS Synth Biol 13:2188–2198. https://doi.org/10.1021/acssynbio.4c00273

Ledesma-Amaro R, Dulermo R, Niehus X, Nicaud J-M (2016) Combining metabolic engineering and process optimization to improve production and secretion of fatty acids. Metab Eng 38:38–46. https://doi.org/10.1016/j.ymben.2016.06.004

Lee S, Jung Y, Lee S, Lee J (2013) Correlations between FAS elongation cycle genes expression and fatty acid production for improvement of long-chain fatty acids in *Escherichia coli*. Appl Biochem Biotechnol 169:1606–1619. https://doi.org/10.1007/s12010-012-0088-8

Lennen RM, Pfleger BF (2012) Engineering *Escherichia coli* to synthesize free fatty acids. Trends Biotechnol 30:659–667. https://doi.org/10.1016/j.tibtech.2012.09.006

Lennen RM, Braden DJ, West RM, Dumesic JA, Pfleger BF (2010) A process for microbial hydrocarbon synthesis: overproduction of fatty acids in *Escherichia coli* and catalytic conversion to alkanes. Biotechnol Bioeng 106:193–202. https://doi.org/10.1002/bit.22660

Lennen RM, Kruziki MA, Kumar K, Zinkel RA, Burnum KE, Lipton MS, Hoover SW, Ranatunga DR, Wittkopp TM, Marner WD, Pfleger BF (2011) Membrane stresses induced by overproduction of free fatty acids in *Escherichia coli*. Appl Environ Microb 77:8114–8128. https://doi.org/10.1128/AEM.05421-11

Li Z, Nimtz M, Rinas U (2014) The metabolic potential of *Escherichia coli* BL21 in defined and rich medium. Microb Cell Fact 13:45. https://doi.org/10.1186/1475-2859-13-45

Liu X, An Y, Gao H (2024) Engineering cascade biocatalysis in whole cells for syringic acid bioproduction. Microb Cell Fact 23:162. https://doi.org/10.1186/s12934-024-02441-x

Lu Q, Inouye M (1996) Adenylate kinase complements nucleoside diphosphate kinase deficiency in nucleotide metabolism. Proc Natl Acad Sci USA 93:5720–5725. https://doi.org/10.1073/pnas.93.12.5720

Lu Q, Zhang X, Almaula N, Mathews CK, Inouye M (1995) The gene for nucleoside diphosphate kinase functions as a mutator gene in *Escherichia coli*. J Mol Biol 254:337–341. https://doi.org/10.1006/jmbi.1995.0620

Lu Q, Li J, Wang J, Li K, Li J, Han P, Chen P, Zhou W (2017) Exploration of a mechanism for the production of highly unsaturated fatty acids in *Scenedesmus* sp. at low temperature grown on oil crop residue based medium. Bioresource Technol 244:542–551. https://doi.org/10.1016/j.biortech.2017.08.005

Matthay P, Schalck T, Verstraeten N, Michiels J (2023) Strategies to enhance the biosynthesis of monounsaturated fatty acids in *Escherichia coli*. Biotechnol Bioproc E. https://doi.org/10.1007/s12257-022-0295-2

Millar G, Lewendon A, Hunter MG, Coggins JR (1986) The cloning and expression of the *aroL* gene from *Escherichia coli* K12. Purification and complete amino acid sequence of shikimate kinase II, the *aroL*-gene product. Biochem J 237:427–437. https://doi.org/10.1042/bj2370427

Monk JM, Lloyd CJ, Brunk E, Mih N, Sastry A, King Z, Takeuchi R, Nomura W, Zhang Z, Mori H, Feist AM, Palsson BO (2017) *i*ML1515, a knowledgebase that computes *Escherichia coli* traits. Nat Biotechnol 35:904–908. https://doi.org/10.1038/nbt.3956

Muenwongtham S, Jaturapiree P, Pimviriyakul P (2022) Effect of supplemented sugar in lysogeny broth medium on growth of

Escherichia coli BL21(DE3) and recombinant protein production. Agr Nat Resour 56:537–546

Park S, Kim GB, Kim HU, Park SJ, Choi J (2019) Enhanced production of poly-3-hydroxybutyrate (PHB) by expression of response regulator DR1558 in recombinant *Escherichia coli*. INT J Biol Macromol 131:29–35. https://doi.org/10.1016/j.ijbiomac.2019.03.044

Peskov K, Mogilevskaya E, Demin O (2012) Kinetic modelling of central carbon metabolism in *Escherichia coli*. FEBS J 279:3374–3385. https://doi.org/10.1111/j.1742-4658.2012.08719.x

Pfleger BF, Gossing M, Nielsen J (2015) Metabolic engineering strategies for microbial synthesis of oleochemicals. Metab Eng 29:1–11. https://doi.org/10.1016/j.ymben.2015.01.009

Pharkya P, Burgard AP, Maranas CD (2003) Exploring the overproduction of amino acids using the bilevel optimization framework OptKnock. Biotechnol Bioeng 84:887–899. https://doi.org/10.1002/bit.10857

Prieto-de Lima TS, Rojas-Jimenez K, Vaglio C (2024) Strategy for optimizing vitamin B12 production in *Pseudomonas putida* KT2440 using metabolic modeling. Metabolites 14:636. https://doi.org/10.3390/metabo14110636

Ranganathan S, Tee TW, Chowdhury A, Zomorrodi AR, Yoon JM, Fu Y, Shanks JV, Maranas CD (2012) An integrated computational and experimental study for overproducing fatty acids in *Escherichia coli*. Metab Eng 14:687–704. https://doi.org/10.1016/j.ymben.2012.08.008

Reisch CR, Prather KLJ (2015) The no-SCAR (Scarless Cas9 Assisted Recombineering) system for genome editing in *Escherichia coli*. Sci Rep 5:15096. https://doi.org/10.1038/srep15096

Rodriguez A, Martnez JA, Flores N, Escalante A, Gosset G, Bolivar F (2014) Engineering *Escherichia coli* to overproduce aromatic amino acids and derived compounds. Microb Cell Fact 13:126. https://doi.org/10.1186/s12934-014-0126-z

Roisin MP, Kepes A (1978) Nucleosidediphosphate kinase of *Escherichia coli*, a periplasmic enzyme. Biochimica et Biophysica Acta (BBA) - Enzymol 526:418–428. https://doi.org/10.1016/0005-2744(78)90133-X

Sanders TAB (2009) Fat and fatty acid intake and metabolic effects in the human body. Ann Nutr Metab 55:162–172. https://doi.org/10.1159/000229001

Sezonov G, Joseleau-Petit D, D'Ari R (2007) *Escherichia coli* physiology in Luria-Bertani broth. J Bacteriol 189:8746–8749. https://doi.org/10.1128/JB.01368-07

Tao H, Bausch C, Richmond C, Blattner FR, Conway T (1999) Functional genomics: expression analysis of *Escherichia coli* growing on minimal and rich media. J Bacteriol 181:6425–6440. https://doi.org/10.1128/JB.181.20.6425-6440.1999

Veit A, Polen T, Wendisch VF (2007) Global gene expression analysis of glucose overflow metabolism in *Escherichia coli* and reduction of aerobic acetate formation. Appl Microbiol Biotechnol 74:406–421. https://doi.org/10.1007/s00253-006-0680-3

Voelker T, Davies H (1994) Alteration of the specificity and regulation of fatty acid synthesis of *Escherichia coli* by expression of a plant medium-chain acyl-acyl carrier protein thioesterase. J Bacteriol 176:7320–7327. https://doi.org/10.1128/jb.176.23.7320-7327.1994

Voelker T, Worrell A, Anderson L, Bleibaum J, Fan C, Hawkins D, Radke S, Davies H (1992) Fatty acid biosynthesis redirected to medium chains in transgenic oilseed plants. Science 257:72–74. https://doi.org/10.1126/science.1621095

Wang J, Tan H, Zhao Z, (Kent), (2007) Over-expression, purification, and characterization of recombinant NAD-malic enzyme from *Escherichia coli* K12. Protein Expres Purif 53:97–103. https://doi.org/10.1016/j.pep.2006.11.017

Whipp MJ, Pittard AJ (1995) A reassessment of the relationship between *aroK*- and *aroL*-encoded shikimate kinase enzymes of *Escherichia coli*. J Bacteriol 177:1627–1629. https://doi.org/10.1128/jb.177.6.1627-1629.1995

Wilmaerts D, Dewachter L, De Loose P-J, Bollen C, Verstraeten N, Michiels J (2019) HokB monomerization and membrane repolarization control persister awakening. Mol Cell 75:1031–1042

Xiao Y, Ruan Z, Liu Z, Wu SG, Varman AM, Liu Y, Tang YJ (2013) Engineering *Escherichia coli* to convert acetic acid to free fatty acids. Biochem Eng J 76:60–69. https://doi.org/10.1016/j.bej.2013.04.013

Xie X, Liang Y, Liu H, Liu Y, Xu Q, Zhang C, Chen N (2014) Modification of glycolysis and its effect on the production of L-threonine in *Escherichia coli*. J Ind Microb Biotechnol 41:1007–1015. https://doi.org/10.1007/s10295-014-1436-1

Yim H, Haselbeck R, Niu W, Pujol-Baxley C, Burgard A, Boldt J, Khandurina J, Trawick JD, Osterhout RE, Stephen R, Estadilla J, Teisan S, Schreyer HB, Andrae S, Yang TH, Lee SY, Burk MJ, Van Dien S (2011) Metabolic engineering of *Escherichia coli* for direct production of 1,4-butanediol. Nat Chem Biol 7:445–452. https://doi.org/10.1038/nchembio.580

Yu T, Zhou YJ, Huang M, Liu Q, Pereira R, David F, Nielsen J (2018) Reprogramming yeast metabolism from alcoholic fermentation to lipogenesis. Cell 174:1549-1558.e14. https://doi.org/10.1016/j.cell.2018.07.013

Zhang DM, Zhang S, Steichen D (2004) New process for the production of branched-chain fatty acids. J Surfactants Deterg 7:211–215. https://doi.org/10.1007/s11743-004-0306-x

Zhang X, Tervo CJ, Reed JL (2016) Metabolic assessment of *E. coli* as a biofactory for commercial products. Metab Eng 35:64–74. https://doi.org/10.1016/j.ymben.2016.01.007

Zhao C, Lin Z, Dong H, Zhang Y, Li Y (2017) Reexamination of the physiological role of PykA in *Escherichia coli* revealed that it negatively regulates the intracellular ATP levels under anaerobic conditions. Appl Environ Microbiol 83:e00316-e317. https://doi.org/10.1128/AEM.00316-17

Zhao C, Dong H, Zhang Y, Li Y (2019) Discovery of potential genes contributing to the biosynthesis of short-chain fatty acids and lactate in gut microbiota from systematic investigation in *E. coli*. npj Biofilms Microbiomes 5:19. https://doi.org/10.1038/s41522-019-0092-7